Evaluating the mobility of polymer-stabilised zero-valent iron nanoparticles and their potential to co-transport contaminants in intact soil cores

L. Chekli, [a, b, #] G. Brunetti, [b, c, #] E. R. Marzouk, [c, d] A. Maoz-Shen, [b, c] E. Smith, [b, c] R. Naidu, [b, e] H.K. Shon, [a, b] E. Lombi [c] and E. Donner [b, c, *]

[a] School of Civil and Environmental Engineering, University of Technology, Sydney, Post Box 129, Broadway, NSW 2007, Australia.

[b] Cooperative Research Centre for Contamination Assessment and Remediation of the Environment, ATC Building, University of Newcastle, Callaghan, NSW 2308, Australia.

[c] Future Industries Institute, University of South Australia, Building X, Mawson Lakes Campus, SA 5095, Australia.

[d] Division of Soil and Water Sciences, Faculty of Environmental Agricultural Sciences, Suez Canal University, North Sinai 45516, Egypt.

[e] Global Centre for Environmental Remediation (GCER), Faculty of Science and Information Technology, University of Newcastle, Callaghan, NSW 2308, Australia.

[*]Corresponding author: Email: Erica.Donner@unisa.edu.au; Phone: (+61) 08 8302 3624

[#] L.C. and G.B. equally contributed to this work.

ABSTRACT

The use of zero-valent iron nanoparticles (nZVI) has been advocated for the remediation of both soils and groundwater. A key parameter affecting nZVI remediation efficacy is the mobility of the particles as this influences the reaction zone where remediation can occur. However, by engineering nZVI particles with increased stability and mobility we may also inadvertently facilitate nZVI-mediated contaminant transport away from the zone of treatment. Previous nZVI mobility studies have often been limited to model systems (e.g. sand columns) as the presence of background Fe makes detection and tracking of nZVI in real systems difficult. Here, we overcame this problem by synthesising Fe-59 radiolabelled nZVI. This approach enabled us to detect and quantify the leaching of nZVI-derived Fe-59 in intact soil cores, including a soil contaminated by Chromated-Copper-Arsenate (CCA). Mobility of a commercially available nZVI was also tested. The results showed limited mobility of both nanomaterials with less than 1% of the injected mass eluted from the columns and most of the radiolabelled nZVI remaining in the surface soil layers (the primary treatment zone in this CCA contaminated soil). Nevertheless, the observed breakthrough of contaminants and nZVI occurred simultaneously, indicating that although the quantity transported was low in this case, nZVI does have the potential to co-transport contaminants. These results show that direct injection of nZVI into the surface layers of contaminated soils may be a viable remediation option for soils such as this one, in which the mobility of nZVI below the zone of injection/remediation was very limited. The Fe-59 experimental approach demonstrated here can be further extended to test nZVI transport in a wider range of contaminated soil types and textures and using different application methods and rates. The resulting database could then be used to develop and validate modelling of nZVI-facilitated contaminant transport on an individual soil basis suitable for site specific risk assessment prior to nZVI remediation.

Keywords: Zero-valent iron, nanoparticles, mobility, CMC, radiolabeling, isotope

Capsule: The synthesis of Fe-59 radiolabelled nZVI enabled detection and quantification of nZVI and nZVI-facilitated contaminant transport in intact soil cores containing natural iron colloids.

1 Introduction

To date, nanoscale zero-valent iron (nZVI) particles have been the most widely used and researched engineered nanoparticles (ENPs) for environmental remediation (Tratnyek and Johnson 2006, EPA 2008, Karn et al. 2009, Mueller et al. 2012). Various studies have demonstrated the high performance of nZVI for the degradation, removal or stabilisation of a range of contaminants; including chlorinated organic solvents (Elliott and Zhang 2001, Zhang 2003, Liu et al. 2005, Liu and Lowry 2006, Phenrat et al. 2009, Kim et al. 2010, Fan et al. 2015) as well as redox sensitive inorganic contaminants (Alowitz and Scherer 2002, Kanel et al. 2005, Kanel et al. 2007, Dorjee et al. 2014, Dong et al. 2016, Li et al. 2016, Yadav et al. 2016) such as arsenic (As), chromium (Cr), and antimony (Sb). Although nZVI is most frequently examined for its potential application in subsurface environments such as contaminated aquifers (Mueller et al. 2012), it has also shown promise as a remediation option for contaminated surface soils and has been tested in a variety of treatment scenarios in both *ex situ* and *in situ* treatment formats (e.g. (Satapanajaru et al. 2008, Yuan et al. 2012, El-Temsah and Joner 2013, Dorjee et al. 2014, Di Palma et al. 2015)). For example, Mele et al. (2015) found that direct addition of nZVI to a highly contaminated mine site soil significantly decreased both *in vivo* Pb bioavailability (mouse model) and As bioaccessibility (SBRC gastric and intestinal phases), indicating that the addition of nZVI as a soil amendment could potentially reduce the human and environmental health risks associated with mining-impacted soils.

One of the most commonly cited challenges to the more widespread utilisation of nZVI for *in situ* remediation is its limited mobility in natural porous systems. This is mainly due to particle aggregation and sedimentation, and related problems such as pore blocking and deposition of nZVI onto the granular porous matrices. Together, these processes can limit the effectiveness of *in situ* remediation (Schrick et al. 2004, Quinn et al. 2005, He and Zhao

2007, Saleh et al. 2008). This has made nZVI mobility a topic of current research focus. However, although increasing the mobility of nZVI is desirable in order to maximise the zone of remediation influence, it also increases the possibility for undesirable side-effects; in particular, the potential for nZVI to adsorb and transport contaminants away from the primary zone of contamination (Mueller and Nowack 2009, Dong and Lo 2014). Previous research has demonstrated enhanced transport of low-solubility contaminants by naturally occurring nanoparticles (i.e. colloids) (de Jonge et al. 2004) and the ability of nZVI to sorb soil contaminants has already been reported for As, Cr and other inorganic contaminants (Schorr 2007). Together, these findings suggest that nZVI application could, in some cases, promote the subsurface movement and dispersion of contaminants; a possibility that requires further assessment.

Many studies have focused on the use of surface modifiers such as polymers, polyelectrolytes or surfactants to decrease the aggregation and deposition of nZVI and enhance particle mobility (De Gennes 1987). Surface modification provides electrostatic and/or steric forces that counter the strong inter-particle magnetic attractive forces and thereby increase colloidal stabilisation (Wiesner and Bottero 2007). Various surface modifiers have been proposed to improve nZVI stability, including carboxymethyl cellulose (CMC) (e.g. (Kocur et al. 2012, Raychoudhury et al. 2012, Basnet et al. 2013, Jung et al. 2014, Raychoudhury et al. 2014)), poly(acrylic acid) (PAA) (e.g. (Jiemvarangkul et al. 2011, Laumann et al. 2013, Laumann et al. 2014)), poly(styrenesulfonate) (PSS) (Phenrat et al. 2008, Cirtiu et al. 2011), sodium dodecylbenzenesulfonate (SDBS) (Saleh et al. 2007, Saleh et al. 2008) and triblock copolymer (Saleh et al. 2007, Saleh et al. 2008, Kim et al. 2012). Many studies have demonstrated reduced aggregation and/or improved transport in saturated porous media when polymers, polyelectrolytes or surfactants are used to stabilise nZVI suspension (e.g. (He et al. 2007, Saleh et al. 2007, Phenrat et al. 2008, Saleh et al. 2008, Tiraferri et al. 2008, Tiraferri

and Sethi 2009, Cirtiu et al. 2011, Basnet et al. 2013, Laumann et al. 2014, Raychoudhury et al. 2014)).

However, most studies investigating nZVI transport have been carried out in ideal systems consisting of repacked, homogeneous, coarse textured porous media (e.g. (Kocur et al. 2012, Raychoudhury et al. 2012, Basnet et al. 2013, Raychoudhury et al. 2014)) or even glass beads (e.g. (Kanel et al. 2007, Lin et al. 2010, Busch et al. 2014)). Furthermore, cleaning and drying procedures are often used to remove both metallic and organic impurities (e.g. (Raychoudhury et al. 2012, Basnet et al. 2013)). These "ideal" conditions are not necessarily representative of natural conditions, but do facilitate the detection and quantification of nZVI mobility by reducing the background Fe content. By contrast, relatively few studies have considered the heterogeneity of natural porous media and focused on the individual or combined effects of different physical and chemical components in order to understand factors affecting the mobility of nZVI (e.g. the effect of pH, natural organic matter (NOM), clay content, etc.). These studies showed that the presence of NOM can enhance the mobility of polymer-stabilised nZVI due to repulsive electrosteric forces between the NOM macromolecules and the negatively-charged surface coating (Johnson et al. 2009, Jung et al. 2014). Kim et al. (2012) demonstrated that at pH 6-8, there was greater deposition of CMC-nZVI onto clay minerals due to the charge heterogeneity on clay mineral surfaces, while Laumann et al. (2013) found reduced mobility of PAA-nZVI in the presence of carbonate minerals.

Options for *in situ* soil remediation using nZVI include direct surface soil injection. As such, it is important to assess the mobility of polymer-stabilised nZVI in intact soil cores and its potential to co-transport contaminants (an undesirable potential side-effect). This knowledge could significantly help in the development of effective remediation materials and methods, and also in risk assessment. However, this task remains extremely challenging due to the high

122 background of natural iron (Fe) colloids present in soils and other environmental systems.
123 This impasse can potentially be overcome by labelling the ENPs in order to differentiate them
124 from natural colloids. This approach can make the ENP of interest easily detectable, even in
125 complex matrices containing relevant concentrations of environmental nanoparticles (Zänker
126 and Schierz 2012). Possible labelling methods for ENP tracking include fluorescence
127 labelling (where a dye is attached to the surface of the ENPs (Kirchner et al. 2005)),
128 radiolabeling with γ or β emitters (Ferguson et al. 2008, Oughton et al. 2008, Petersen et al.
129 2008, Abbas et al. 2010, Gibson et al. 2011, Hildebrand and Franke 2012), and isotope
130 labelling with stable isotopes (Gulson and Wong 2006, Croteau et al. 2011, Dybowska et al.
131 2011). The labelling process can either be performed directly during the nanoparticle
132 synthesis by using a labelled precursor or via post-synthesis manipulation (Zänker and
133 Schierz 2012), but labelling during synthesis is preferable.

134 The overall objectives of this study were:

135 1. To synthesise radiolabelled ^{59}Fe-CMC-nZVI and investigate its mobility and that of
136 commercially available PAA-nZVI in intact soil cores. The mobility of the
137 commercial nZVI was investigated using an ICP-MS method while ^{59}Fe-CMC-nZVI
138 mobility was assessed by gamma counting.

139 2. To determine the retention profiles of radiolabelled nZVI in the soil columns after the
140 mobility experiments.

141 3. To assess the potential of nZVI to co-transport contaminants in chromated-copper-
142 arsenate (CCA)-contaminated soil by coupling gamma counting and ICP-MS
143 measurements.

To the authors' knowledge, this is the first time that radiolabelling has been used to investigate a) the mobility of nZVI in intact soil cores, and b) the potential for nZVI to act as a vector for contaminant transport.

2 Materials and methods

2.1 Commercial N25S and ^{59}Fe-CMC-nZVI synthesis

Commercial NANOFER 25S (N25S) was supplied by NANOIRON, s.r.o. (Czech Republic) in the form of a slurry with a mean primary particle diameter < 50 nm and total iron concentration of 20 % (w/w) (as provided by the manufacturer). These iron particles are modified by an inorganic iron oxide layer and an organic PAA coating as described by Kadar et al. (2011). Prior to the experiments, a freshly received stock solution was prepared under anoxic conditions with a final concentration of 50 g/L and sealed in a glass bottle.

CMC-nZVI was synthesised according to the methods described by Lin et al. (2010) and Cirtiu et al. (2011). The isotopic labelling was done during the first stage of the synthesis by spiking 160 µL (260 MBq) of $^{59}FeCl_3$ solution (Perkin Elmer, radionuclide purity of 99%, specific activity: 1623.88 MBq/mL) into 800 mL of 0.125 M $FeSO_4.7H_2O$ (Sigma Aldrich, Australia) solution. The resulting specific activity of the labelled nZVI was 61.5 Bq/mg. This solution was then mixed for 5 minutes before adding 800 mL of a 1.75% (w/v) Na-CMC (90 K, Sigma Aldrich, Australia) solution which was mixed thoroughly for 30 minutes. $NaBH_4$ (Sigma Aldrich, Australia) solution was then added drop wise at a rate of 5 mL/min under an anoxic atmosphere. The ratio of $[Fe^{2+}]/[BH_4^-]$ was set at 1:2. The mixture was stirred for an additional 30 minutes. The final nZVI solution was sealed in a bottle under anoxic conditions and mixed at 135 rpm on a shaker overnight.

In order to remove the excess chemicals from the synthesis product, the final nZVI solution was placed on a magnet for 5 hours to settle, and the supernatant was then discarded and replaced with degassed and deionised water. This purification process was repeated three times to obtain a concentrated "purified" stock solution containing a negligible concentration of free CMC. The recovery rate was determined by analysing both the supernatant and the stock solution with a gamma radiation counter (2480 Wizard^2-3, Perkin Elmer). The recovery was 81% and the final stock solution concentration was adjusted to 50 g/L.

Detailed characterisation (i.e. morphology, elemental composition, particle size distribution and specific activity for the ^{59}Fe-CMC-nZVI) of both nanoparticle suspensions used in these experiments is provided in the Supporting Information.

2.2 Column transport experiments

2.2.1 Soil type and experimental design

Two South Australian topsoils (0-15 cm) were collected for this study; an uncontaminated sandy-loam soil from Mount Compass (intact soil cores extracted onsite) and a CCA-contaminated sandy-loam soil collected from a timber storage area in the Barossa Valley (intact soil cores extracted onsite). CCA has been widely employed worldwide as a wood preservative to expand the lifespan of treated wooden structures exposed to weather (Hingston et al. 2001). Various studies have, however, demonstrated that the CCA metals/metalloids may leach when the treated wood is exposed to environmental conditions. This ultimately results in elevated concentrations of Cr, copper (Cu), and As in the surrounding environment of the CCA-treated wooden structure (Hopp et al. 2008).

The physico-chemical characteristics of both soils are provided in the Supporting Information (Table S2). From this point forward, the two topsoils will be designated as MC and CCA soils.

190 Soil corers made of PVC were 15 cm long with an inner diameter of 10 cm. A nylon mesh
191 (200 μm) was secured over the bottom of the column after removal from the soil profile to
192 hold the soil in place. The soil columns were first saturated from below for 24 hours using
193 artificial soil pore water (Glæsner et al. 2012) and then drained and equilibrated overnight to
194 ensure similar initial conditions for all columns. The soil cores were then connected to an
195 irrigation system in which peristaltic pumps (Masterflex L/S, Cole Palmer, Australia) were
196 used to ensure a constant flow rate of 1 mm/hr throughout the experiments. This low rate is
197 common for extended rainfall events in South Australia (Glæsner et al. 2012). Artificial
198 rainwater (Oorts et al. 2007) was used for leaching in this study. Baseline experiments (i.e.
199 prior to injecting nZVI) were conducted for three days and leachates from the baseline study
200 were collected regularly and stored in the dark at 4°C until analysed. After the 3-day baseline
201 establishment period the irrigation was stopped for 2 hours; nZVI was then applied to the
202 columns by sub-surface injection. The nZVI suspensions (i.e. 50 g/L stock solution) were
203 spiked into the top of the columns, simultaneously applying the nZVI to each column through
204 a bundle of 19 uniformly spaced and equally filled 10 mL syringes. The nZVI was thus
205 injected into the uppermost 2 cm of the soil (representing about 200 g of soil considering a
206 soil density of 1.3 g/cm^3) at the beginning of each experiment at an application rate of 1%
207 (w/w) (i.e. approximately 2 g of nZVI injected per column) which is comparable with the
208 application rates used in previous studies involving nZVI application to metal contaminated
209 soil (Lombi et al. 2002, Kim et al. 2009, Mele et al. 2015). The irrigation system was started
210 immediately after the injection of nZVI and leaching experiments were conducted for a
211 further three days. A tracer test using potassium bromide (KBr) was conducted
212 simultaneously with KBr (40 mg/L) added to the artificial rainwater at the beginning of the
213 experiment immediately after nZVI addition. The bottom of each column was connected to a
214 funnel in which the leachates were collected continuously. Each funnel was connected to an

auto-sampler (peristaltic pump) collecting approximately 20-50 mL of the leachates at predetermined time intervals (i.e. every three hours on the first day and then twice a day for the rest of the experiment). Leachates were filtered through 0.2 μm filters (Regenerated cellulose, Thermofisher) and effluent bromide concentrations were analysed by ion chromatography (Dionex ICS 2000, Thermo Scientific, CA, USA).

2.2.2 Evaluation of commercialised N25S mobility by means of ICP-MS-based total Fe analysis

As described above, 2 g of N25S were injected into the top of the MC soil columns before re-starting the irrigation system. Four soil columns were used for this experiment; three replicate columns to which nZVI was added and one control column to determine the background Fe concentration in the MC soil (in addition to the baseline data collection for each column which also determined this). The collected effluent samples were acid digested and Fe concentration was determined using inductively coupled plasma mass spectrometry (ICP-MS) (Agilent 8800 Triple Quadrupole, Agilent Technologies, CA, USA). The data presented are the average of replicate experiments (n = 3).

2.2.3 Gamma counting method to test mobility of ^{59}Fe-CMC- nZVI

The mobility of radiolabelled nZVI was assessed in both MC and CCA soils. Three replicate columns of each soil were used for the transport study and data presented are the average of replicate measurements (n = 3). ^{59}Fe-CMC-nZVI (i.e. 2 g nZVI containing 0.123 MBq or 2,072K counts per minutes (CPM)) was added on top of each column and 2 ml aliquots of the collected effluent samples were analysed directly using a gamma radiation counter (2480 Wizard^2-3, Perkin Elmer) without any further sample preparation. Replicate sample tubes containing blank solutions (i.e. MilliQ water) were included in each rack of samples analysed on the gamma counter in order to determine the relevant background radiation, and this

239 background value was subsequently subtracted from the results obtained for the effluent
240 samples measured in that rack. For this study, no control columns were needed as the gamma
241 counter only detects the gamma emission from the radiolabelled ^{59}Fe-nZVI. This is one of the
242 main advantages of this method as the background of naturally occurring Fe colloids present
243 in the columns does not interfere with the results. The mass of eluted nZVI was calculated by
244 measuring the activity in solution (adjusted to Time 0 – taking into consideration the
245 radionuclide decay) and using the specific activity of the nZVI (i.e. at Time 0).

246 To investigate the effect of wetting and drying on the mobility of nZVI, the irrigation system
247 was stopped for one month after the first set of experiments and then started again for three
248 consecutive days. Effluent samples were collected at the same frequency as for the first set of
249 experiments and analysed directly with the gamma radiation counter.

250 Following the completion of the experiments, each column was dissected into different layers
251 to determine the spatial distribution profile of retained nZVI. This gave a total of 10 soil layer
252 samples, with a 1 cm section for the top layer, 1.5 cm section for the underlying layer, and
253 2.5 cm sections in the lower layers. Preliminary experiments were first conducted to assess
254 the activity attenuation of each of the soil types compared to water, and the results (Figure
255 S7, SI) showed that for the highest concentrations tested, the attenuation was less than 10 %.
256 Therefore, three replicate soil samples (32 grams) were extracted from each layer and
257 analysed directly with the gamma radiation counter (i.e. without any sample preparation).
258 This is another advantage of this method over conventional elemental composition analysis
259 (e.g. ICP-MS), which would have required sample preparation in the form of acid digestion
260 and would not have differentiated between the injected nZVI and the natural Fe already
261 present in the soil columns.

2.2.4 Co-transport of contaminants in CCA-contaminated soil

Eluted samples from the CCA soil columns were also acid digested and elemental concentrations of Fe, Cr, copper (Cu) and (As) were determined by ICP-MS. For this experiment, the initial leaching period (i.e. baseline study prior to adding nZVI) was used as control data for each column due to the heterogeneity in contaminant concentration between the different replicate columns. Leachates from the baseline study were acid digested and analysed with ICP-MS to determine the background concentration of Fe, Cr, Cu and As prior to the injection of nZVI. The data presented are the average of replicate measurements (n = 3).

3 Results and discussion

3.1 Evaluating the mobility of commercial N25S mobility by means of ICP-MS-based total Fe analysis

The mobility of N25S was assessed in MC soil columns for 72 hours after injection of the N25S and the results are presented in Figure 1 and Table S3 (SI).

The conservative tracer (i.e. KBr) breakthrough curve, shown in Figure 1a, indicated steady state effluent concentration by the end of the experiments suggesting that non-equilibrium processes, such as rate-limited mass transfer into regions of immobile water or preferential flow paths, were not significant during the transport of nZVI in the soil columns.

Figure 1b shows that the mass of Fe eluted from the control column (i.e. without N25S) was fairly steady (i.e. 0.42 mg ± 0.06 mg) while the mass of Fe eluted from the spiked columns increased slowly, up to a maximum around 25 hours, and then slowly decreased until the end of the experiments. It is worth noting that the mass of Fe leached from the control column was quite low and steady throughout the experiment. This supports the assumption that the

enhanced Fe elution in the N25S treated column was due to the movement of nZVI, even though this cannot be unequivocally proved by simply analysing the eluent with ICP-MS. Currently, ICP-MS would typically need to be coupled with another instrument to detect the presence of nanoparticles, and these other possible techniques (e.g. microscopy) are not quantitative and therefore not statistically relevant (Chekli et al. 2016). Single particle ICP-MS analysis could be a useful technique to apply in order to detect the presence of nanoparticles but this method is still relatively new and has not yet been optimised for Fe analysis. Importantly, we also note that in the case of a soil with higher and/or unevenly distributed Fe elution, standard ICP-MS would not be sensitive enough to detect the spiked engineered nanomaterials eluted from the soil. This was thus the basis for proposing the method of isotopic labelling to circumvent this challenge.

The experimental breakthrough curve for N25S, shown in Figure 1c, indicates that only a small fraction of the initial injected mass was eluted from the MC soil columns (i.e. m/m_0 was less than 0.0004 at 25 hours); suggesting that most of the nZVI particles were retained in the column. Mass balance calculations, presented in Table S3 (SI), confirmed that less than 20 mg of N25S were eluted after 72 hours which represents less than 1% of the injected mass (2 g).

Figure 1

There are several effects which can explain the limited transport behaviour of N25S: the ripening effect, which occurs when the system is dominated by colloid-colloid attraction forces (i.e. aggregation) and whereby attached particles can act as additional anchors for attachment by forming multilayer films (Rajagopalan and Chu 1982, Ryde et al. 1991, Liu et al. 1995); the straining effect - when the particles are trapped in down-gradient pore throats that are too small to allow particle passage (McDowell-Boyer et al. 1986); and deposition of the charged nanoparticles onto soil grains with opposite charge (i.e. sorption) (Phenrat et al.

2010). Straining would cause the deposition of particles to decrease gradually since the smaller pores contributing to straining would fill up with time and restrict the other particles to larger pore networks, leading to an increase in effluent Fe concentration. In this study, the eluted mass of Fe was not increasing with time as expected in the case of straining (Figure 1b). However, straining cannot be excluded as it may be possible that not all of the smaller pores had reached saturation by the end of these experiments. A ripening effect due to the aggregation of nanoparticles is likely to have contributed to restricting the mobility of N25S in this study. Even though surface modifiers were employed to reduce the aggregation of nZVI there may have still been some residual aggregation (Phenrat et al. 2008, Fatisson et al. 2010, Raychoudhury et al. 2012), particularly given the relatively high particle concentration (i.e. 50 g/L) used (Phenrat et al. 2009). Finally, the sorption of polymer-coated nZVI onto soil grains through electrostatic attraction forces has been shown to significantly decrease its mobility (Liu et al. 1995, Fatisson et al. 2010, Kim et al. 2012, Raychoudhury et al. 2012, Laumann et al. 2013, Jung et al. 2014), and sorption of the nZVI by soil constituents is likely even though the nanoparticles were negatively charged, as even though the net charge of the soil was slightly negative (Table S2), a number of anions are known to be sorbed in sub-acidic soils. It is therefore very probable that all three processes (i.e. straining, aggregation and sorption) contributed to limiting the mobility of nZVI.

3.2 Evaluating the mobility of radiolabelled CMC-nZVI using gamma counting

3.2.1 Transport of ^{59}Fe-CMC-nZVI in MC soil columns

The mobility of radiolabelled CMC-nZVI was first assessed in MC soil columns. After an initial leaching period of 72 hours (similar to the N25S mobility study), the columns were left to dry for one month. The irrigation system was then started again for 72 hours to assess the

effect of the drying/wetting cycle on the mobility of nZVI. Results are presented in Figure 2 and Table S4 (SI).

The KBr tracer breakthrough (Figure 2a) was slightly delayed in comparison to the KBr breakthrough obtained in Figure 1a but, by the end of the 3 days the eluent concentrations approached C_0.

Similarly to the behaviour of N25S, experimental breakthrough of CMC-nZVI (Figure 2b-d) indicated limited mobility of the nanomaterials in the MC soil columns (i.e. m/m_0 was less than 0.0004 throughout the experiment). In replicate columns 2 and 3, however, some of the nanomaterials eluted very quickly, within a few minutes after the injection (i.e. $m/m_0 > 0.001$ - Figure 2 c and 2d), which is most likely related to preferential flows. Dissection revealed that these preferential flows mainly originated from heterogeneities in the soil such as cracks, gravels, soil organisms (i.e. earthworm, insect larvae, etc.), root holes and macropores. No notable sidewall effects were observed during the experiments; this was confirmed at the end of the experiment during the column sectioning as nZVI preferential pathways are clearly visible in the form of iron oxidation products if present (data not shown).

Results from the mass balance calculation in Table S4 (SI) confirmed that most of the particles (i.e. more than 98.9% of the total injected mass) were retained in the columns. Results in Table S4 (SI) also show the higher eluted mass in both columns 2 and 3 (i.e. about 3 mg eluted from column 1 compared to 20.99 mg and 14.81 mg from columns 2 and 3 respectively). Without considering the effect of preferential flows (i.e. excluding results from replicate columns 2 and 3), the mass of nZVI eluted from the MC soil columns was higher for N25S (i.e. about 20 mg compared to 5 mg for CMC-nZVI – Tables S3 and S4, SI). This is in accordance with a previous study by Lin et al. (2010) where they found that the mobility of PAA-nZVI was superior to CMC-nZVI.

Figure 2

It has been demonstrated in previous studies that hydrodynamic perturbation such as rapid infiltration, episodic wetting and drying cycles or large increases in shear stress can cause the detachment of colloidal particles from solid minerals (Saiers and Lenhart 2003, Zhuang et al. 2007). In the present study, Figure 2b-d show that wetting and drying events did not have any appreciable effect on the mobility of nZVI as the mass eluted during the second leaching period remained significantly low (i.e. less than 1 mg). This could be due to the fact that aggregates of nZVI had become trapped in down-gradient pore throats which restricted their subsequent mobility, and/or degradation of the coating agents and oxidation of the nZVI core as this would have promoted particle retention.

After completion of the mobility study, all three columns were dissected into 10 layers in order to determine the distribution of the nZVI retained in the columns (Figure 3). More detailed information, such as the mass of nZVI recovered from the dissected columns, can be found in Table S5 (SI). Results indicate that about 40 to 65% of the retained particles remained in the first few centimetres; which is most probably related to the processes described above. The retention profiles of ^{59}Fe-CMC-nZVI in all three columns exhibit a hyperexponential shape with higher retention in the layers next to the column inlet and rapidly decreasing retention with depth. Hyperexponential retention profiles have also been observed in previous studies investigating the transport of nanoparticles in porous media (Wang et al. 2011, Liang et al. 2013). Previous studies have suggested that hyperexponential retention profiles can be due to straining (Li et al. 2004), particle aggregation (Bradford et al. 2006), system hydrodynamics (Bradford et al. 2011, Liang et al. 2013) or surface charge heterogeneity on the porous media grains (Tufenkji and Elimelech 2005). It is likely that all these processes have contributed to some extent toward this result.

In both columns 2 and 3, some particles (i.e. about 5% of the total mass recovered) were found in the deepest layers; which confirms the early elution of particles in these two columns due to preferential flows.

Figure 3

3.2.2 Transport of ^{59}Fe-CMC-nZVI in CCA-contaminated soil columns

The transport of radiolabelled CMC-nZVI in the CCA soil columns was also assessed and the results are presented in Figure 4 and Table S4 (SI). Similar to the behaviour in MC soil columns, ^{59}Fe-CMC-nZVI showed very poor mobility in CCA soil columns (i.e. $m/m_0 <$ 0.00015-0.0004 - Figure 4b-d) with less than 0.5% (i.e. 10 mg) of the injected mass eluted from the columns (Table S4, SI). The breakthrough curves of ^{59}Fe-CMC-nZVI were almost identical in both soils with increasing mass eluted, up to a peak occurring at about 18 hours, and then slowly decreasing to the end of the first leaching period. The second leaching period (i.e. after the columns were left to dry for one month) showed no enhancement in particle mobility; which is similar to the trend observed in the MC soil columns.

Figure 4

The retention profiles of ^{59}Fe-CMC-nZVI in the CCA soil columns were similar to those observed in the MC soil columns; exhibiting a hyperexponential shape. Figure 5 shows that more than 90% of the particles were retained in the top centimetre of the columns; confirming the low mobility of the particles. This value rapidly decreased to 5-10% in the following layers (i.e. up to 5 cm deep) and less than 0.5% in the deepest layers.

Figure 5

3.3 Co-transport of contaminants in CCA-contaminated soil

The potential for nZVI to co-transport inorganic contaminants was assessed using the CCA soil columns and the results are presented in Figure 6. For this experiment, the baseline data

405 from the initial leaching period (i.e. prior to adding nZVI) was used as control data for each
406 column. This was preferable to using separate control columns for comparison as it helps
407 circumvent confounding effects caused by heterogeneity in contaminant concentrations
408 within and between the different replicate columns (i.e. Column 1 released the highest
409 concentration of all three contaminants - Figure 6). Results show that the eluted mass of all
410 three contaminants (i.e. Cr, Cu and As) was increasing with time during the baseline
411 establishment period, suggesting that some of the contaminants were present in the mobile
412 aqueous phase, either in dissolved form or bound to natural colloids. In fact, many previous
413 studies focusing on contaminant transport in porous media demonstrated that contaminants
414 are partitioned between an immobile solid phase (i.e. bound to immobile matrix), a mobile
415 aqueous phase and a mobile colloidal phase (Massoudieh and Ginn 2010). The eluted mass of
416 Fe during the baseline study was quite stable and homogeneous between the three replicate
417 columns. After the injection of nZVI, the eluted mass of all three contaminants continued to
418 increase for a short period of time and then gradually decreased. This may indicate that
419 contaminants were effectively adsorbed on the surface of nZVI which reduced their mobility.
420 In fact, many studies have already demonstrated that nZVI may be effective for the treatment
421 of both Cr and As (Dries et al. 2005, Kanel et al. 2005, Kanel et al. 2007, Schorr 2007,
422 Ramos et al. 2009). In these studies, it was reported that nZVI can reduce both the mobility
423 and toxicity of inorganic contaminants following surface-adsorption and/or a change in
424 speciation induced by redox reactions. However, this implies that the contaminants remain in
425 the environment but are changed to a less mobile and/or less toxic form.

426 After decreasing, the eluted mass of all three contaminants began to increase again, up to a
427 peak at about 18 hours which corresponds to the peak observed for Fe in both Figure 6 (i.e.
428 ICP-MS results) and Figure 4 (i.e. gamma counter results). This may indicate the effective
429 transport of contaminants following their adsorption on the surface of nZVI. Ryan and

Elimelech (1996) suggested that the following three criteria should be present for the effect of colloid-facilitated contaminant transport to be important: (i) colloids should be present in large enough concentration, (ii) the contaminant should be adsorbed to the colloids and (iii) the colloids should be mobile in the porous medium. As the eluted mass of all three contaminants was much lower (i.e. in the μg range - Figure 6) than the injected mass of nZVI (i.e. 2 g), and previous studies have already demonstrated that nZVI can effectively adsorbed metals, both criteria (i) and (ii) for colloid-facilitated transport are met. However, we have demonstrated that the mobility of ^{59}Fe-CMC-nZVI in the CCA soil columns was very limited and that most of the retained particles were present in the top first centimetres of the columns. Nonetheless, the mass of eluted Fe from nZVI (i.e. about 3-7 mg) remained higher than the eluted mass of contaminants (i.e. less than 100 μg) which may indicate the effective transport of all three contaminants by the eluted nZVI.

Finally, as discussed in the previous section, the wetting/drying cycle did not have any effect on the mobility of nZVI or the three contaminants. Figure 6 shows that the eluted mass of Cr, Cu, As and Fe was fairly steady and quite low during the second leaching period.

Figure 6

Conclusions

The main objective of this study was to demonstrate the feasibility of a novel Fe-59 labelling method enabling the detection and quantification of nZVI in natural soils containing significant Fe backgrounds. One of the objectives was also to demonstrate that, by coupling this method with ICP-MS, it is possible to assess the potential of nZVI to co-transport contaminants.

The results obtained in this research have several implications. First, compared to previous research carried out in simplified model systems (e.g. sand), the results of the present study showed very little translocation of polymer-coated nZVI in intact soil cores. The retention profiles of retained particles showed that most of the particles remained in the top layers of the soil profile demonstrating that nZVI injected into the surface layers of a contaminated soil may be a viable remediation approach with limited associated risk of increased facilitated transport of contaminants to the subsoil. In fact, the concentration of contaminants in the eluent after nZVI application were similar to those obtained in the pre-treatment phase indicating that the potential for contaminant mobilisation appears to be low, at least in the soil investigated here and under the injection conditions tested. Nevertheless, in cases where direct surface soil injection of nZVI is combined with ploughing and mixing, or alternatively, where *ex situ* treatment and soil replacement is considered, a greater degree of nZVI/colloidal facilitated contaminant transport may be expected and further research is needed to understand the extent of this.

It is important to note that the radiolabelled nanoparticles used in this study were produced for research purposes in order to overcome some of the inherent challenges in studying the mechanisms and processes of nZVI remediation in complex soil systems. This method is

suitable for further use in lab testing but it is not suggested for use directly in field application studies due to the use of radioisotopes. Future studies should focus on applying this method to a wider range of soil types and contaminants in order to establish a database for modelling studies with the eventual goal of facilitating validated modelling of nZVI-facilitated contaminant transport on an individual soil basis suitable for site specific risk assessment prior to nZVI remediation.

Supporting Information

Additional text, tables, and figures containing information about the characteristics of the nanomaterials and soil used, retention profiles, summary of the dissection experiments and selected results from data analyses not presented in the main text.

Acknowledgements

This research was funded by the Cooperative Research Centre for Contamination Assessment and Remediation of the Environment (CRC CARE). Support was provided to EL, ED and HS by the Australian Research Council (ARC) through Future Fellowships (FT100100337; FT130101003 and FT140101208) and to EL through project DP110103174.

References

Abbas, K., I. Cydzik, R. Del Torchio, M. Farina, E. Forti, N. Gibson, U. Holzwarth, F. Simonelli and W. Kreyling, 2010. Radiolabelling of TiO2 nanoparticles for radiotracer studies. Journal of Nanoparticle Research 12, 2435-2443.

Alowitz, M. J. and M. M. Scherer, 2002. Kinetics of nitrate, nitrite, and Cr(vi) reduction by iron metal. Environmental Science and Technology 36, 299-306.

Basnet, M., S. Ghoshal and N. Tufenkji, 2013. Rhamnolipid biosurfactant and soy protein act as effective stabilizers in the aggregation and transport of palladium-doped zerovalent iron nanoparticles in saturated porous media. Environmental Science and Technology 47, 13355-13364.

Bradford, S. A., J. Simunek and S. L. Walker, 2006. Transport and straining of E. coli O157: H7 in saturated porous media. Water Resources Research 42, W12S12.

Bradford, S. A., S. Torkzaban and J. Simunek, 2011. Modeling colloid transport and retention in saturated porous media under unfavorable attachment conditions. Water Resources Research 47, W10503.

Busch, J., T. Meißner, A. Potthoff and S. E. Oswald, 2014. Transport of carbon colloid supported nanoscale zero-valent iron in saturated porous media. Journal of Contaminant Hydrology 164, 25-34.

Chekli, L., B. Bayatsarmadi, R. Sekine, B. Sarkar, A. M. Shen, K. Scheckel, W. Skinner, R. Naidu, H. Shon and E. Lombi, 2016. Analytical characterisation of nanoscale zero-valent iron: A methodological review. Analytica Chimica Acta 903, 13-35.

Cirtiu, C. M., T. Raychoudhury, S. Ghoshal and A. Moores, 2011. Systematic comparison of the size, surface characteristics and colloidal stability of zero valent iron nanoparticles pre- and post-grafted with common polymers. Colloids and Surfaces A: Physicochemical and Engineering Aspects 390, 95-104.

Croteau, M.-N., A. D. Dybowska, S. N. Luoma and E. Valsami-Jones, 2011. A novel approach reveals that zinc oxide nanoparticles are bioavailable and toxic after dietary exposures. Nanotoxicology 5, 79-90.

De Gennes, P., 1987. Polymers at an interface; a simplified view. Advances in Colloid and Interface Science 27, 189-209.

de Jonge, L. W., C. Kjærgaard and P. Moldrup, 2004. Colloids and Colloid-Facilitated Transport of Contaminants in Soils An Introduction. Vadose Zone Journal 3, 321-325.

Di Palma, L., M. Gueye and E. Petrucci, 2015. Hexavalent chromium reduction in contaminated soil: a comparison between ferrous sulphate and nanoscale zero-valent iron. Journal of Hazardous Materials 281, 70-76.

Dong, H., K. Ahmad, G. Zeng, Z. Li, G. Chen, Q. He, Y. Xie, Y. Wu, F. Zhao and Y. Zeng, 2016. Influence of fulvic acid on the colloidal stability and reactivity of nanoscale zero-valent iron. Environmental Pollution 211, 363-369.

Dong, H. and I. M. C. Lo, 2014. Transport of Surface-Modified Nano Zero-Valent Iron (SM-NZVI) in saturated porous media: Effects of surface stabilizer type, subsurface geochemistry, and contaminant loading. Water, Air, and Soil Pollution 225, 2107.

Dorjee, P., D. Amarasiriwardena and B. Xing, 2014. Antimony adsorption by zero-valent iron nanoparticles (nZVI): Ion chromatography–inductively coupled plasma mass spectrometry (IC–ICP-MS) study. Microchemical Journal 116, 15-23.

Dries, J., L. Bastiaens, D. Springael, S. Kuypers, S. N. Agathos and L. Diels, 2005. Effect of humic acids on heavy metal removal by zero-valent iron in batch and continuous flow column systems. Water Research 39, 3531-3540.

534 Dybowska, A. D., M.-N. Croteau, S. K. Misra, D. Berhanu, S. N. Luoma, P. Christian, P.
535 O'Brien and E. Valsami-Jones, 2011. Synthesis of isotopically modified ZnO nanoparticles
536 and their potential as nanotoxicity tracers. Environmental Pollution 159, 266-273.
537 El-Temsah, Y. S. and E. J. Joner, 2013. Effects of nano-sized zero-valent iron (nZVI) on
538 DDT degradation in soil and its toxicity to collembola and ostracods. Chemosphere 92, 131-
539 137.
540 Elliott, D. W. and W. X. Zhang, 2001. Field assessment of nanoscale bimetallic particles for
541 groundwater treatment. Environmental Science and Technology 35, 4922-4926.
542 EPA, U. S., 2008. Nanotechnology for site remediation fact sheet.
543 Fan, W., Y. Cheng, S. Yu, X. Fan and Y. Deng, 2015. Preparation of wrapped nZVI particles
544 and their application for the degradation of trichloroethylene (TCE) in aqueous solution.
545 Journal of Water Reuse and Desalination 5, 335-343.
546 Fatisson, J., S. Ghoshal and N. Tufenkji, 2010. Deposition of carboxymethylcellulose-coated
547 zero-valent iron nanoparticles onto silica: Roles of solution chemistry and organic molecules.
548 Langmuir 26, 12832-12840.
549 Ferguson, P. L., G. T. Chandler, R. C. Templeton, A. DeMarco, W. A. Scrivens and B. A.
550 Englehart, 2008. Influence of sediment− amendment with single-walled carbon nanotubes
551 and diesel soot on bioaccumulation of hydrophobic organic contaminants by benthic
552 invertebrates. Environmental Science & Technology 42, 3879-3885.
553 Gibson, N., U. Holzwarth, K. Abbas, F. Simonelli, J. Kozempel, I. Cydzik, G. Cotogno, A.
554 Bulgheroni, D. Gilliland and J. Ponti, 2011. Radiolabelling of engineered nanoparticles for in
555 vitro and in vivo tracing applications using cyclotron accelerators. Archives of Toxicology
556 85, 751-773.
557 Glæsner, N., E. Donner, J. Magid, G. H. Rubæk, H. Zhang and E. Lombi, 2012.
558 Characterization of leached phosphorus from soil, manure, and manure-amended soil by
559 physical and chemical fractionation and diffusive gradients in thin films (DGT).
560 Environmental Science and Technology 46, 10564-10571.
561 Gulson, B. and H. Wong, 2006. Stable isotopic tracing: A way forward for nanotechnology.
562 Environmental health perspectives 1486-1488.
563 He, F. and D. Zhao, 2007. Manipulating the size and dispersibility of zerovalent iron
564 nanoparticles by use of carboxymethyl cellulose stabilizers. Environmental Science and
565 Technology 41, 6216-6221.
566 He, F., D. Zhao, J. Liu and C. B. Roberts, 2007. Stabilization of Fe - Pd nanoparticles with
567 sodium carboxymethyl cellulose for enhanced transport and dechlorination of
568 trichloroethylene in soil and groundwater. Industrial and Engineering Chemistry Research 46,
569 29-34.
570 Hildebrand, H. and K. Franke, 2012. A new radiolabeling method for commercial Ag0
571 nanopowder with 110mAg for sensitive nanoparticle detection in complex media. Journal of
572 Nanoparticle Research 14, 1-7.
573 Hingston, J., C. Collins, R. Murphy and J. Lester, 2001. Leaching of chromated copper
574 arsenate wood preservatives: a review. Environmental Pollution 111, 53-66.
575 Hopp, L., P. S. Nico, M. A. Marcus and S. Peiffer, 2008. Arsenic and chromium partitioning
576 in a podzolic soil contaminated by chromated copper arsenate. Environmental Science &
577 Technology 42, 6481-6486.
578 Jiemvarangkul, P., W. X. Zhang and H. L. Lien, 2011. Enhanced transport of polyelectrolyte
579 stabilized nanoscale zero-valent iron (nZVI) in porous media. Chemical Engineering Journal
580 170, 482-491.
581 Johnson, R. L., G. O. B. Johnson, J. T. Nurmi and P. G. Tratnyek, 2009. Natural organic
582 matter enhanced mobility of nano zerovalent iron. Environmental Science and Technology
583 43, 5455-5460.

584 Jung, B., D. O'Carroll and B. Sleep, 2014. The influence of humic acid and clay content on
585 the transport of polymer-coated iron nanoparticles through sand. Science of the Total
586 Environment 496, 155-164.
587 Kadar, E., G. A. Tarran, A. N. Jha and S. N. Al-Subiai, 2011. Stabilization of engineered
588 zero-valent nanoiron with Na-acrylic copolymer enhances spermiotoxicity. Environmental
589 Science & Technology 45, 3245-3251.
590 Kanel, S. R., B. Manning, L. Charlet and H. Choi, 2005. Removal of arsenic(III) from
591 groundwater by nanoscale zero-valent iron. Environmental Science and Technology 39,
592 1291-1298.
593 Kanel, S. R., D. Nepal, B. Manning and H. Choi, 2007. Transport of surface-modified iron
594 nanoparticle in porous media and application to arsenic (III) remediation. Journal of
595 Nanoparticle Research 9, 725-735.
596 Karn, B., T. Kuiken and M. Otto, 2009. Nanotechnology and in situ remediation: a review of
597 the benefits and potential risks. Environmental health perspectives 1823-1831.
598 Kim, H., H.-J. Hong, J. Jung, S.-H. Kim and J.-W. Yang, 2010. Degradation of
599 trichloroethylene (TCE) by nanoscale zero-valent iron (nZVI) immobilized in alginate bead.
600 Journal of Hazardous Materials 176, 1038-1043.
601 Kim, H. J., T. Phenrat, R. D. Tilton and G. V. Lowry, 2012. Effect of kaolinite, silica fines
602 and pH on transport of polymer-modified zero valent iron nano-particles in heterogeneous
603 porous media. Journal of colloid and interface science 370, 1-10.
604 Kim, K.-R., G. Owens and R. Naidu, 2009. Heavy metal distribution, bioaccessibility, and
605 phytoavailability in long-term contaminated soils from Lake Macquarie, Australia. Soil
606 Research 47, 166-176.
607 Kirchner, C., T. Liedl, S. Kudera, T. Pellegrino, A. Muñoz Javier, H. E. Gaub, S. Stölzle, N.
608 Fertig and W. J. Parak, 2005. Cytotoxicity of colloidal CdSe and CdSe/ZnS nanoparticles.
609 Nano Letters 5, 331-338.
610 Kocur, C. M., D. M. O'Carroll and B. E. Sleep, 2012. Impact of nZVI stability on mobility in
611 porous media. Journal of Contaminant Hydrology 145, 17-25.
612 Laumann, S., V. Micić and T. Hofmann, 2014. Mobility enhancement of nanoscale zero-
613 valent iron in carbonate porous media through co-injection of polyelectrolytes. Water
614 Research 50, 70-79.
615 Laumann, S., V. Micić, G. V. Lowry and T. Hofmann, 2013. Carbonate minerals in porous
616 media decrease mobility of polyacrylic acid modified zero-valent iron nanoparticles used for
617 groundwater remediation. Environmental Pollution 179, 53-60.
618 Li, S., W. Wang, F. Liang and W.-x. Zhang, 2016. Heavy metal removal using nanoscale
619 zero-valent iron (nZVI): Theory and application. Journal of Hazardous Materials Accepted
620 Manuscript.
621 Li, X., T. D. Scheibe and W. P. Johnson, 2004. Apparent decreases in colloid deposition rate
622 coefficients with distance of transport under unfavorable deposition conditions: A general
623 phenomenon. Environmental Science & Technology 38, 5616-5625.
624 Liang, Y., S. A. Bradford, J. Simunek, M. Heggen, H. Vereecken and E. Klumpp, 2013.
625 Retention and remobilization of stabilized silver nanoparticles in an undisturbed loamy sand
626 soil. Environmental Science & Technology 47, 12229-12237.
627 Lin, Y. H., H. H. Tseng, M. Y. Wey and M. D. Lin, 2010. Characteristics of two types of
628 stabilized nano zero-valent iron and transport in porous media. Science of the Total
629 Environment 408, 2260-2267.
630 Liu, D., P. R. Johnson and M. Elimelech, 1995. Colloid deposition dynamics in flow-through
631 porous media: Role of electrolyte concentration. Environmental Science & Technology 29,
632 2963-2973.

633 Liu, Y. and G. V. Lowry, 2006. Effect of particle age (Fe0 content) and solution pH on NZVI
634 reactivity: H_2 evolution and TCE dechlorination. Environmental Science & Technology 40,
635 6085-6090.
636 Liu, Y., S. A. Majetich, R. D. Tilton, D. S. Sholl and G. V. Lowry, 2005. TCE dechlorination
637 rates, pathways, and efficiency of nanoscale iron particles with different properties.
638 Environmental Science and Technology 39, 1338-1345.
639 Lombi, E., F.-J. Zhao, G. Zhang, B. Sun, W. Fitz, H. Zhang and S. P. McGrath, 2002. In situ
640 fixation of metals in soils using bauxite residue: chemical assessment. Environmental
641 pollution 118, 435-443.
642 Massoudieh, A. and T. R. Ginn, 2010. Colloid-facilitated contaminant transport in
643 unsaturated porous media. Modelling of Pollutants in Complex Environmental Systems 2,
644 263-292.
645 McDowell-Boyer, L. M., J. R. Hunt and N. Sitar, 1986. Particle transport through porous
646 media. Water Resources Research 22, 1901-1921.
647 Mele, E., E. Donner, A. L. Juhasz, G. Brunetti, E. Smith, A. R. Betts, P. Castaldi, S. Deiana,
648 K. G. Scheckel and E. Lombi, 2015. In Situ Fixation of Metal (loid) s in Contaminated Soils:
649 A Comparison of Conventional, Opportunistic, and Engineered Soil Amendments.
650 Environmental Science & Technology 49, 13501-13509.
651 Mueller, N. C., J. Braun, J. Bruns, M. Černík, P. Rissing, D. Rickerby and B. Nowack, 2012.
652 Application of nanoscale zero valent iron (NZVI) for groundwater remediation in Europe.
653 Environmental Science and Pollution Research 19, 550-558.
654 Mueller, N. C. and B. Nowack, 2009. Report on nanotechnology in the technology sector:
655 Environment, European Commission, ObservatoryNano.
656 Oorts, K., U. Ghesquiere and E. Smolders, 2007. Leaching and aging decrease nickel toxicity
657 to soil microbial processes in soils freshly spiked with nickel chloride. Environmental
658 Toxicology and Chemistry 26, 1130-1138.
659 Oughton, D. H., T. Hertel-Aas, E. Pellicer, E. Mendoza and E. J. Joner, 2008. Neutron
660 activation of engineered nanoparticles as a tool for tracing their environmental fate and
661 uptake in organisms. Environmental Toxicology and Chemistry 27, 1883-1887.
662 Petersen, E. J., Q. Huang and J. Weber, Walter J, 2008. Bioaccumulation of radio-labeled
663 carbon nanotubes by Eisenia foetida. Environmental Science & Technology 42, 3090-3095.
664 Phenrat, T., A. Cihan, H. J. Kim, M. Mital, T. Illangasekare and G. V. Lowry, 2010.
665 Transport and deposition of polymer-modified Fe0 nanoparticles in 2-D heterogeneous
666 porous media: Effects of particle concentration, Fe 0 content, and coatings. Environmental
667 Science and Technology 44, 9086-9093.
668 Phenrat, T., H. J. Kim, F. Fagerlund, T. Illangasekare, R. D. Tilton and G. V. Lowry, 2009.
669 Particle size distribution, concentration, and magnetic attraction affect transport of polymer-
670 modified Fe0 nanoparticles in sand columns. Environmental Science & Technology 43,
671 5079-5085.
672 Phenrat, T., Y. Liu, R. D. Tilton and G. V. Lowry, 2009. Adsorbed polyelectrolyte coatings
673 decrease Fe0 nanoparticle reactivity with TCE in water: conceptual model and mechanisms.
674 Environmental science & technology 43, 1507-1514.
675 Phenrat, T., N. Saleh, K. Sirk, H.-J. Kim, R. D. Tilton and G. V. Lowry, 2008. Stabilization
676 of aqueous nanoscale zerovalent iron dispersions by anionic polyelectrolytes: adsorbed
677 anionic polyelectrolyte layer properties and their effect on aggregation and sedimentation.
678 Journal of Nanoparticle Research 10, 795-814.
679 Quinn, J., C. Geiger, C. Clausen, K. Brooks, C. Coon, S. O'Hara, T. Krug, D. Major, W. S.
680 Yoon, A. Gavaskar and T. Holdsworth, 2005. Field demonstration of DNAPL dehalogenation
681 using emulsified zero-valent iron. Environmental Science and Technology 39, 1309-1318.

682 Rajagopalan, R. and R. Q. Chu, 1982. Dynamics of adsorption of colloidal particles in packed
683 beds. Journal of Colloid and Interface Science 86, 299-317.
684 Ramos, M. A., W. Yan, X.-q. Li, B. E. Koel and W.-x. Zhang, 2009. Simultaneous oxidation
685 and reduction of arsenic by zero-valent iron nanoparticles: understanding the significance of
686 the core− shell structure. The Journal of Physical Chemistry C 113, 14591-14594.
687 Raychoudhury, T., N. Tufenkji and S. Ghoshal, 2012. Aggregation and deposition kinetics of
688 carboxymethyl cellulose-modified zero-valent iron nanoparticles in porous media. Water
689 Research 46, 1735-1744.
690 Raychoudhury, T., N. Tufenkji and S. Ghoshal, 2014. Straining of polyelectrolyte-stabilized
691 nanoscale zero valent iron particles during transport through granular porous media. Water
692 Research 50, 80-89.
693 Ryan, J. N. and M. Elimelech, 1996. Colloid mobilization and transport in groundwater.
694 Colloids and Surfaces A: Physicochemical and Engineering Aspects 107, 1-56.
695 Ryde, N., N. Kallay and E. Matijević, 1991. Particle adhesion in model systems. Part 14.—
696 Experimental evaluation of multilayer deposition. Journal of the Chemical Society, Faraday
697 Transactions 87, 1377-1381.
698 Saiers, J. E. and J. J. Lenhart, 2003. Colloid mobilization and transport within unsaturated
699 porous media under transient-flow conditions. Water Resources Research 39, 1019.
700 Saleh, N., H. J. Kim, T. Phenrat, K. Matyjaszewski, R. D. Tilton and G. V. Lowry, 2008.
701 Ionic strength and composition affect the mobility of surface-modified Fe0 nanoparticles in
702 water-saturated sand columns. Environmental Science & Technology 42, 3349-3355.
703 Saleh, N., K. Sirk, Y. Liu, T. Phenrat, B. Dufour, K. Matyjaszewski, R. D. Tilton and G. V.
704 Lowry, 2007. Surface modifications enhance nanoiron transport and NAPL targeting in
705 saturated porous media. Environmental Engineering Science 24, 45-57.
706 Satapanajaru, T., P. Anurakpongsatorn, P. Pengthamkeerati and H. Boparai, 2008.
707 Remediation of atrazine-contaminated soil and water by nano zerovalent iron. Water, Air,
708 and Soil Pollution 192, 349-359.
709 Schorr, J. R., 2007 Promise of Nanomaterials for Water Cleanup. Water Conditioning &
710 Purification.
711 Schrick, B., B. W. Hydutsky, J. L. Blough and T. E. Mallouk, 2004. Delivery vehicles for
712 zerovalent metal nanoparticles in soil and groundwater. Chemistry of Materials 16, 2187-
713 2193.
714 Tiraferri, A., K. L. Chen, R. Sethi and M. Elimelech, 2008. Reduced aggregation and
715 sedimentation of zero-valent iron nanoparticles in the presence of guar gum. Journal of
716 Colloid and Interface Science 324, 71-79.
717 Tiraferri, A. and R. Sethi, 2009. Enhanced transport of zerovalent iron nanoparticles in
718 saturated porous media by guar gum. Journal of Nanoparticle Research 11, 635-645.
719 Tratnyek, P. G. and R. L. Johnson, 2006. Nanotechnologies for environmental cleanup. Nano
720 today 1, 44-48.
721 Tufenkji, N. and M. Elimelech, 2005. Breakdown of colloid filtration theory: Role of the
722 secondary energy minimum and surface charge heterogeneities. Langmuir 21, 841-852.
723 Wang, D., M. Paradelo, S. A. Bradford, W. J. G. M. Peijnenburg, L. Chu and D. Zhou, 2011.
724 Facilitated transport of Cu with hydroxyapatite nanoparticles in saturated sand: Effects of
725 solution ionic strength and composition. Water Research 45, 5905-5915.
726 Wiesner, M. R. and J.-Y. Bottero, 2007. Applications and Impacts of Nanomaterials.
727 Environmental Nanotechnology. New York, The McGraw-Hill Companies.
728 Yadav, R., A. K. Sharma and J. N. Babu, 2016. Sorptive removal of arsenite [As(III)] and
729 arsenate [As(V)] by fuller's earth immobilized nanoscale zero-valent iron nanoparticles (F-
730 nZVI): Effect of Fe0 loading on adsorption activity. Journal of Environmental Chemical
731 Engineering 4, 681-694.

Yuan, S., H. Long, W. Xie, P. Liao and M. Tong, 2012. Electrokinetic transport of CMC-stabilized Pd/Fe nanoparticles for the remediation of PCP-contaminated soil. Geoderma 185–186, 18-25.
Zänker, H. and A. Schierz, 2012. Engineered nanoparticles and their identification among natural nanoparticles. Annual review of analytical chemistry 5, 107-132.
Zhang, W. X., 2003. Nanoscale iron particles for environmental remediation: An overview. Journal of Nanoparticle Research 5, 323-332.
Zhuang, J., J. F. McCarthy, J. S. Tyner, E. Perfect and M. Flury, 2007. In situ colloid mobilization in Hanford sediments under unsaturated transient flow conditions: Effect of irrigation pattern. Environmental Science & Technology 41, 3199-3204.

743 **List of Figures captions**

744

745 **Figure 1:** Summary results of N25S mobility in MC soil columns; (a) Experimental
746 breakthrough curve of KBr; (b) Eluted mass of Fe from control (no nZVI) and spiked
747 columns; (c) Experimental breakthrough curve of N25S. The error bars represent the standard
748 deviation from three replicate columns.

749 **Figure 2:** Summary results of ^{59}Fe-CMC-nZVI mobility in MC soil columns; (a)
750 Experimental breakthrough curve of KBr; (b-d) Experimental breakthrough curve of ^{59}Fe-
751 CMC-nZVI in replicate columns.

752 **Figure 3:** Retention profiles of ^{59}Fe-CMC-nZVI in MC soil columns. The relative mass of Fe
753 is the mass of Fe per layer divided by the sum of the mass in each layer.

754 **Figure 4:** Summary results of ^{59}Fe-CMC-nZVI mobility in CCA soil columns; (a)
755 Experimental breakthrough curve of KBr; (b-d) Experimental breakthrough curve of ^{59}Fe-
756 CMC-nZVI in replicate columns.

757 **Figure 5:** Retention profile of ^{59}Fe-CMC-nZVI in CCA soil columns. The relative mass of Fe
758 is the mass of Fe per layer divided by the sum of the mass in each layer.

759 **Figure 6:** Eluted mass of inorganic contaminants (Cr, Cu and As) and Fe from CCA-soil
760 columns.

761 **List of Figures**

762

763 **Figure 1**

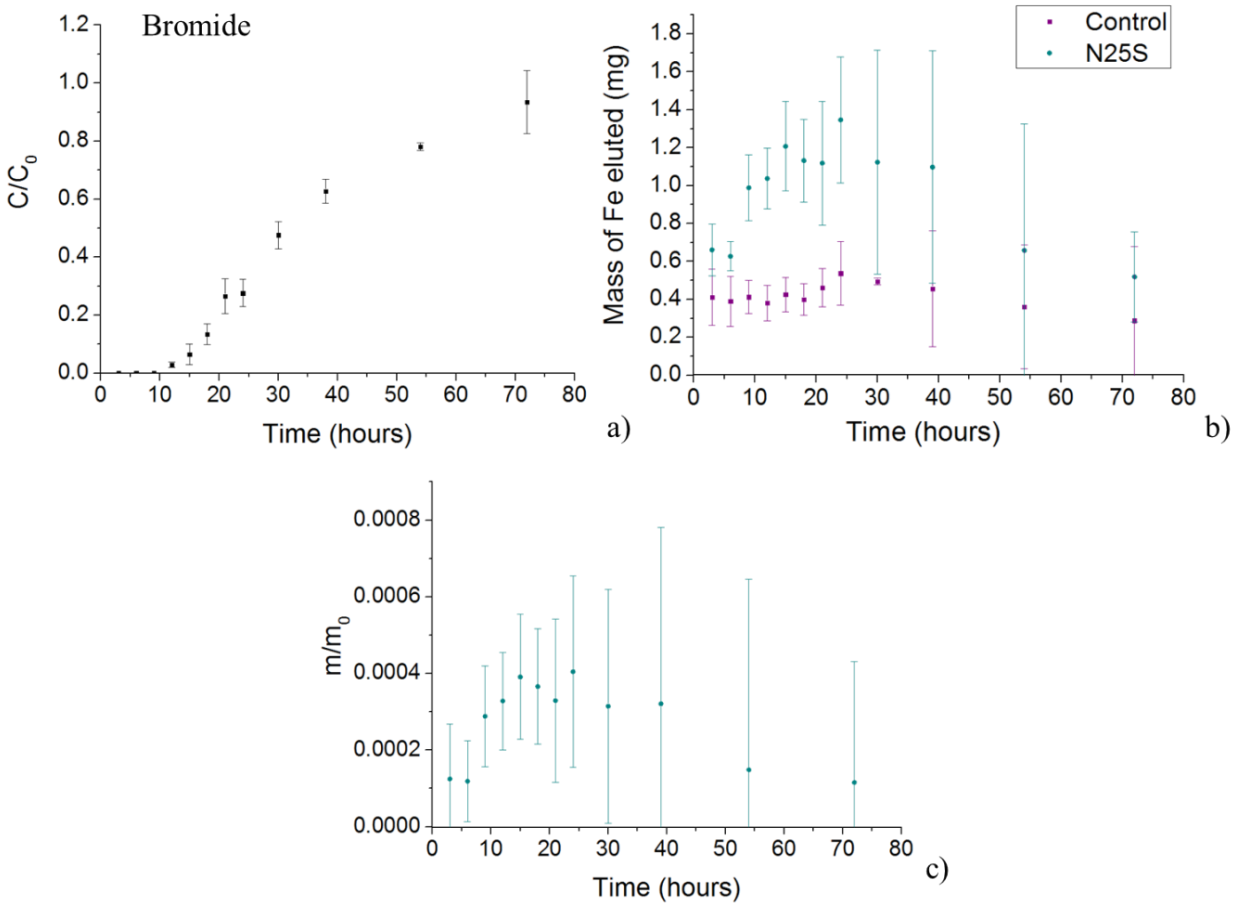

764

765

766 **Figure 2**

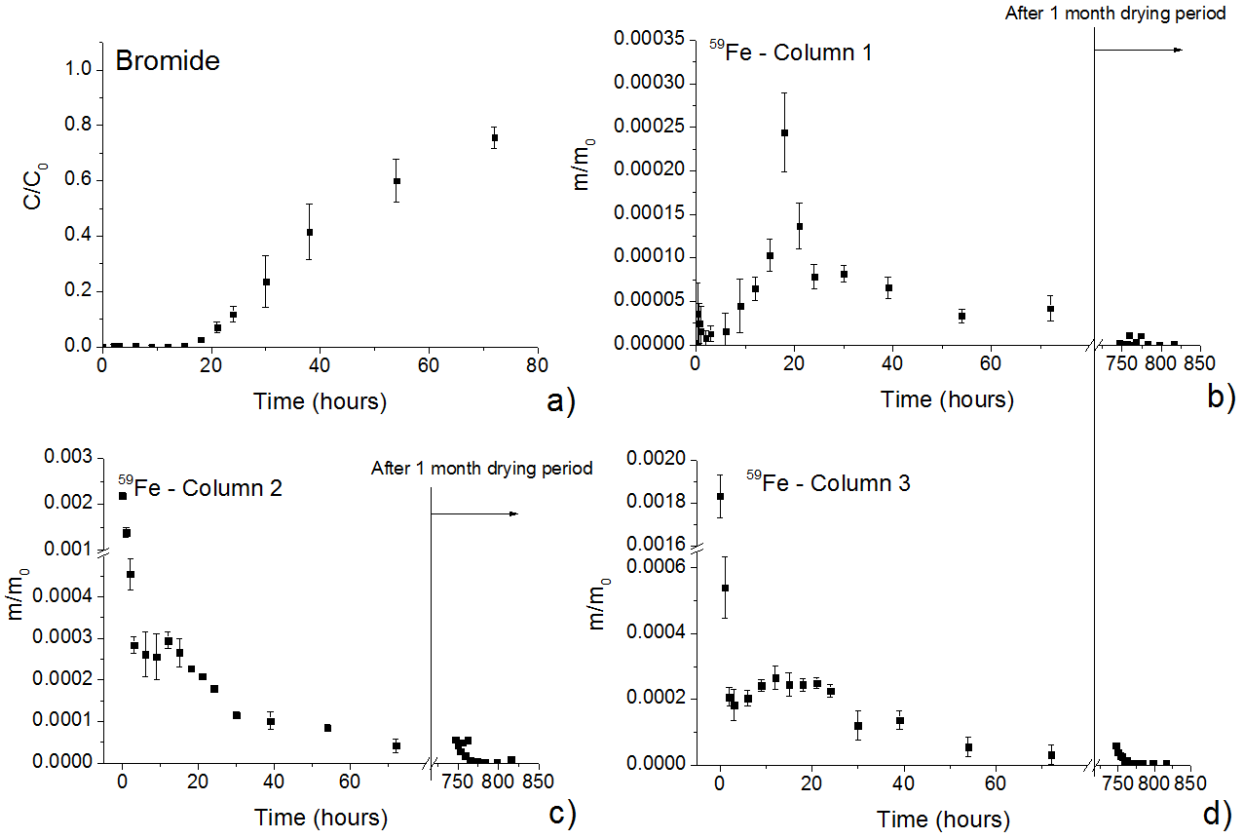

767

768

769 **Figure 3**

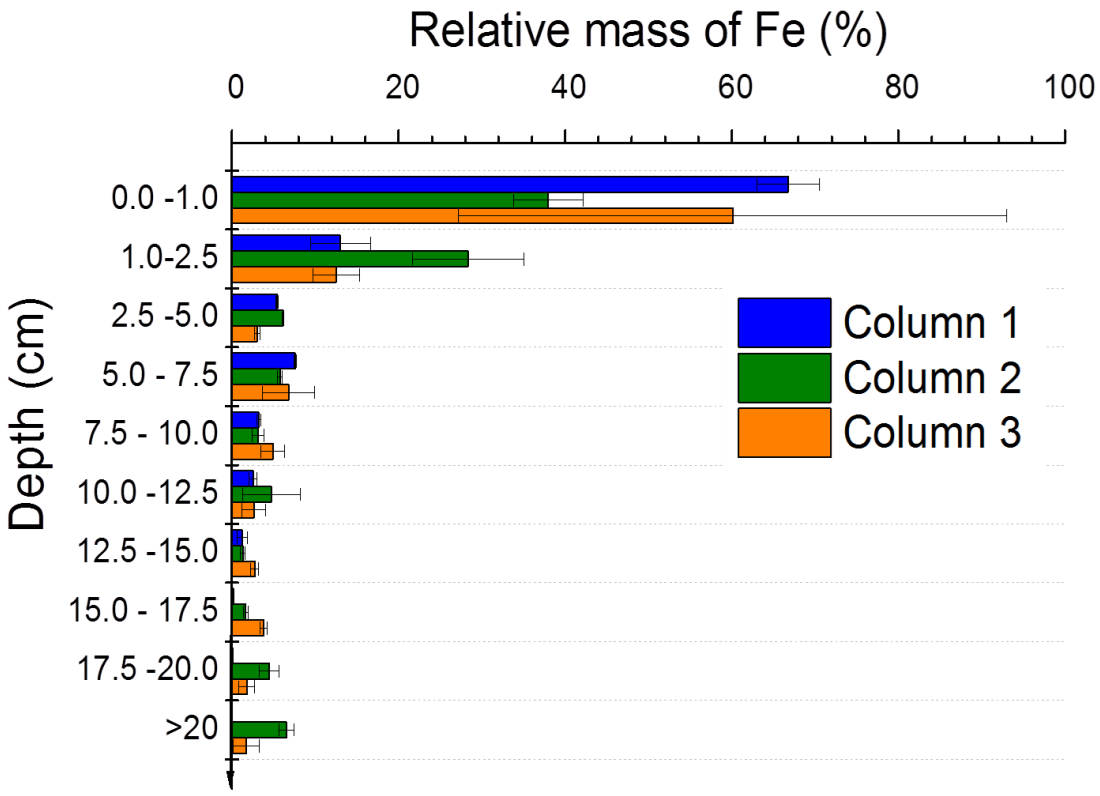

770

771

772 **Figure 4**

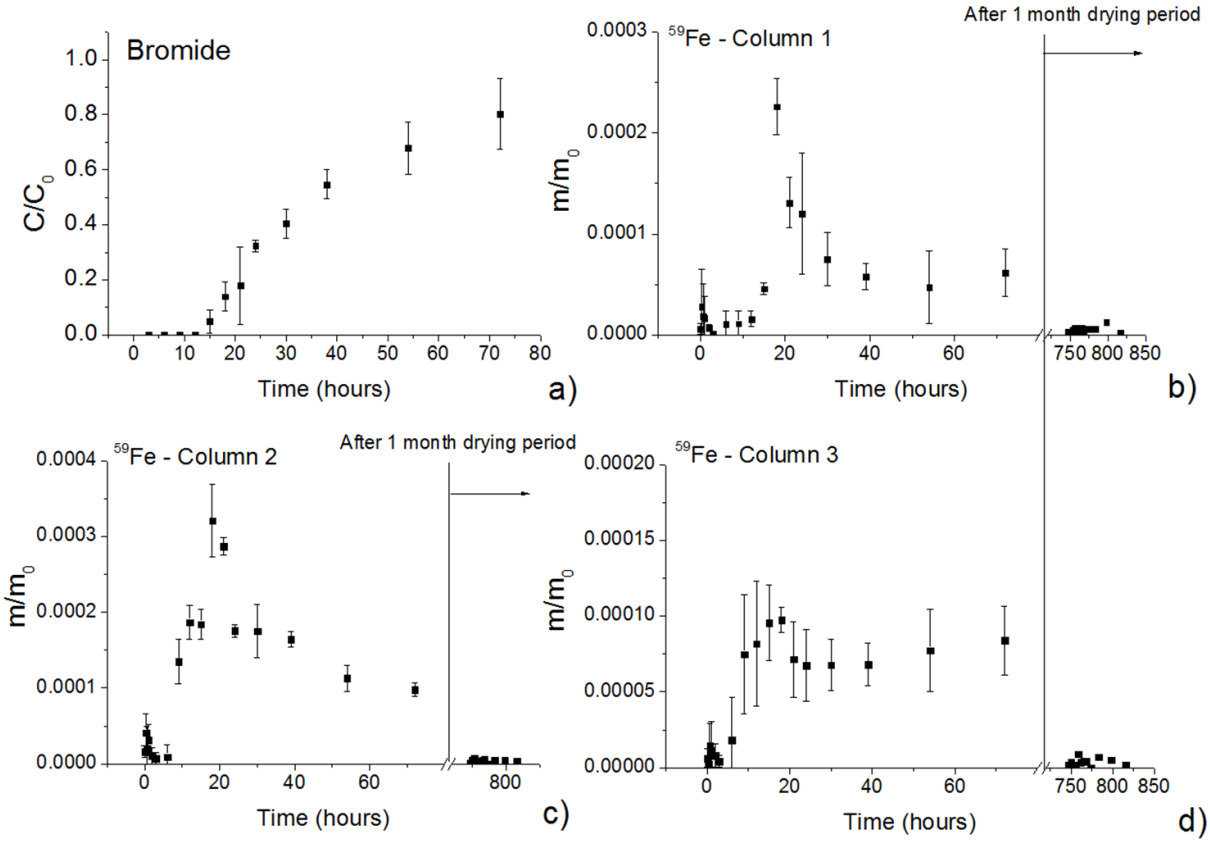

773

774

775 **Figure 5**

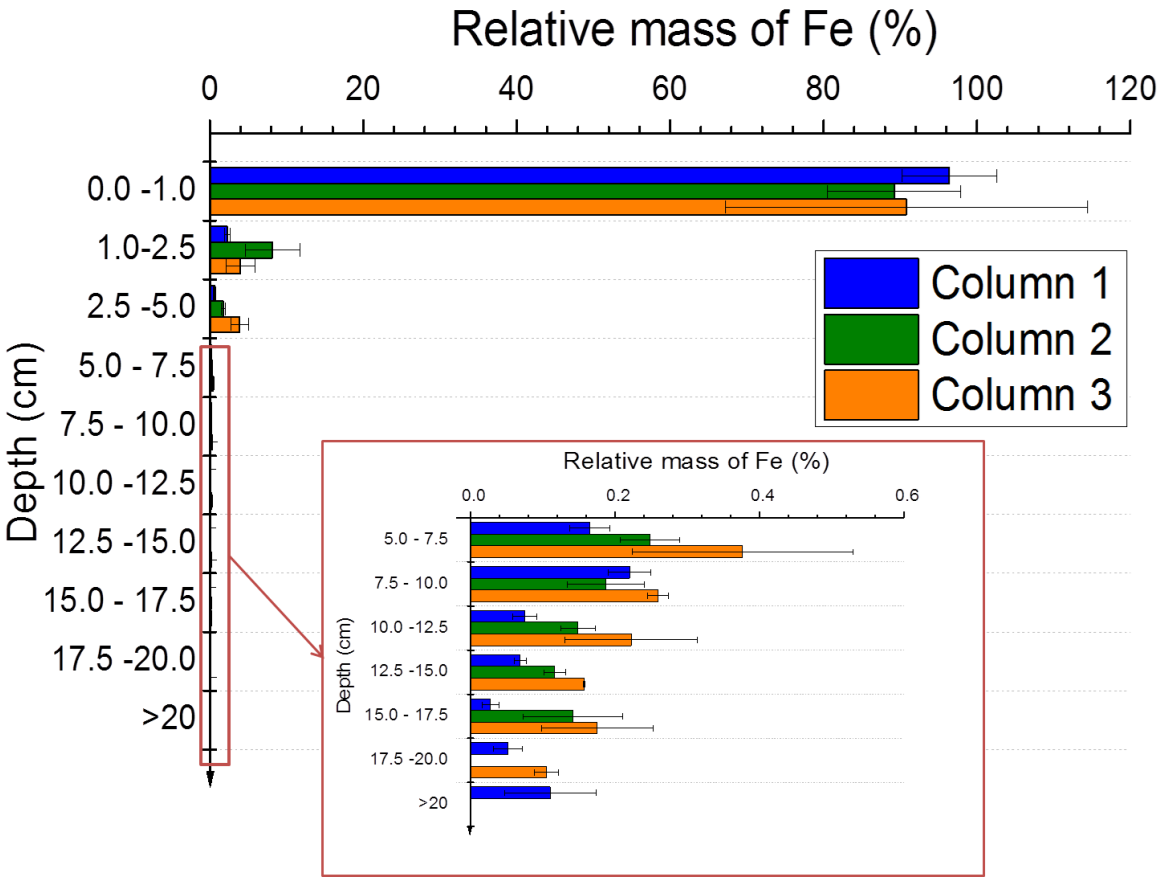

776

777

Figure 6

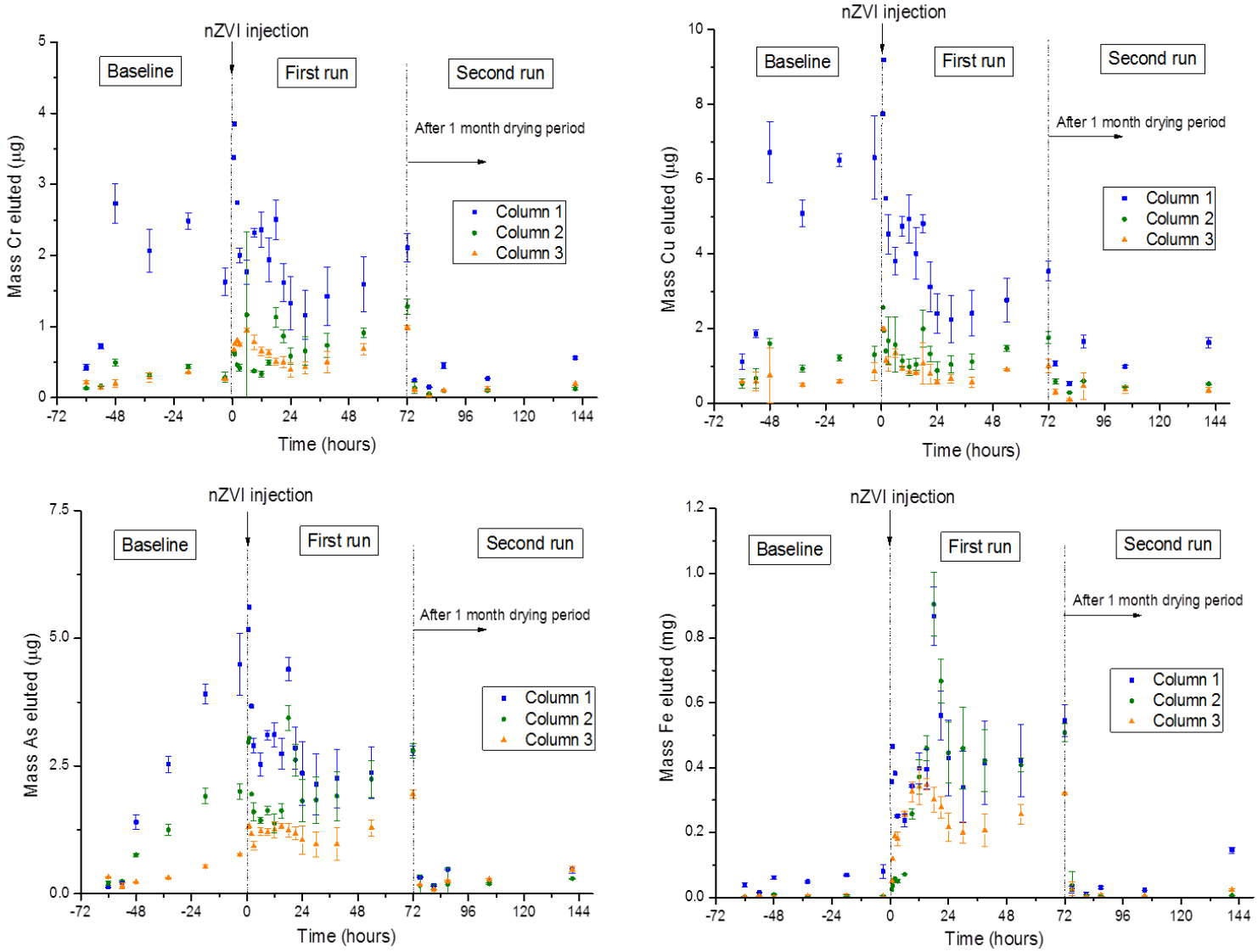
nZVI injection
Baseline
First run
Second run
After 1 month drying period
Column 1
Column 2
Column 3
Mass Cr eluted (µg)
Mass Cu eluted (µg)
Mass As eluted (µg)
Mass Fe eluted (mg)
Time (hours)